Published by :
http://www.ijert.org

International Journal of Engineering Research & Technology (IJERT)
ISSN: 2278-0181
Vol. 13 Issue 4, April 2024

Flexural Testing of Aluminium Alloy 6061: Comparative Analysis of Theoretical Calculations, Finite Element Simulation and Experimental Measurements

He Thong Bui
Department of Mechanical Engineering
The University of Da Nang
University of Technology and Education,
48 Cao Thang, Da Nang, Vietnam

Tuan Phu Vu
Department of Mechanical Engineering
The University of Da Nang
University of Technology and Education,
48 Cao Thang, Da Nang, Vietnam

Van Hoang Vo
Department of Mechanical Engineering
The University of Da Nang
University of Technology and Education,
48 Cao Thang, Da Nang, Vietnam

***Abstract*— In recent years, due to the sharp increase in experimental research in the field of structural engineering, the need to evaluate the reliability of deformation and measurement accuracy has played a very important role. The role of mechanical testing in structural component design is highly significant for verifying the accuracy of computer simulation models and identifying potential weaknesses in designs under both static and dynamic loading conditions. One of the commonly used methods to assess the mechanical properties of materials is the three-point bending method. This article focuses on comparing results obtained through theoretical calculations, finite element simulations, and experimental tests using a low-cost custom-designed 3-point flexural test device. The experiments were set up to measure the deflection of A6061 aluminium alloy samples, and the results obtained were then compared with both theoretical predictions and simulation results. The outcomes of theoretical calculations and simulations demonstrate a high level of accuracy when compared with experimental results, particularly in the elastic deformation region where the A6061 Aluminium samples exhibit linear deformation.**

***Keywords*—three-point bending test; flexural testing; finite element simulation; aluminium alloy 6061; displacement**

I. INTRODUCTION

The increasing prevalence of aluminium alloys in structural applications is not simply a matter of trend, but rather a consequence of their demonstrably advantageous characteristics. These include a notable strength-to-weight ratio, ease of fabrication, high workability, significant ductility, excellent thermal conductivity, strong resistance to corrosion, and an appealing natural finish [1]. The flexural behavior of aluminium alloy columns has been a focal point of research, as it plays a critical role in ensuring the secure transmission of vertical loads to the foundation. Su et al., conducted two sets of 14 three-point bending tests and 15 four-point bending tests on aluminium alloy square and rectangular hollow sections [2]. In recent years, there have been thorough experimental and numerical studies specifically focused on aluminium beams undergoing 3-point [3–5], 4-point [6–8], and 5-point [8] bending conditions. Feng et al., [7] explores the flexural capacity of perforated aluminium CHS tubes, examining two grades: high-strength 6061-T6 and normal-strength 6063-T5 using 3-point and 4-point of bending test. Montuori et al., [3] conducted a finite element study on I-beams made from high-yielding, low-hardening aluminium alloys. Their findings indicated that higher values of the slenderness parameter and shear length ratio lead to a reduction in rotational capacity. It can be noticed that three-point bending test is one of the most common material testing methods to study the mechanical performance of materials. Hou et al., [9] constructed a finite element model to simulate the bending process of specimens with varying punch radii in the three-point bending test, integrating the model data with experimental results. In [10], a numerical analysis is conducted on the three-point test of a simply supported stainless steel beam, and the obtained results are then compared with the experimental data. The utilization of the three-point bending method to examine the deflection behavior of circular-section aluminium beam is scarcely addressed in the literature.

This study investigates the mechanical behavior of aluminium alloy A6061, a versatile material with high strength-to-weight ratio, excellent corrosion resistance, and good machinability, making it widely used in aerospace, automotive, and civil engineering applications. The objective is to assess and compare three methods for predicting the displacement of A6061 3-point bending beams: analytical calculations based on the strength of materials theory, finite element simulations, and experimental measurements using a custom-designed 3-point flexural test device. Through this comparison, the most accurate and efficient approach for predicting the displacement of A6061 beams under bending loads is identified.

International Journal of Engineering Research & Technology (IJERT)
ISSN: 2278-0181
Vol. 13 Issue 4, April 2024

II. EXPERIMENTAL MODEL AND NUMERICAL SIMULATION

A. Development of 3-Point Flexural Test Device

With the aim of accurately and conveniently testing the bending behavior of beams up to 350mm in length, a custom 3-point bending test device was designed and constructed. The device prioritizes three key requirements:

- Versatility: Capable of accommodating beams with a maximum length of 350 mm.
- Accuracy: Delivers reliable and precise displacement measurements.
- Ease of Use: Simple and intuitive operation for efficient testing.

Its components include a robust C45 steel U50 channel chassis for stability and minimal deflection, two parallel steel rails guiding the vertical movement of the loading block to ensure controlled force application, a cylindrical loading block (d = 8 mm) for transmitting the bending load to the beam with vertical movement for precise positioning, and two adjustable cylindrical supports (d = 10 mm) allowing customization of the span length to suit different beam specimens. This custom test device is tailored to meet the specific requirements of versatility, accuracy, and ease of use for comprehensive bending behavior analysis of beams.

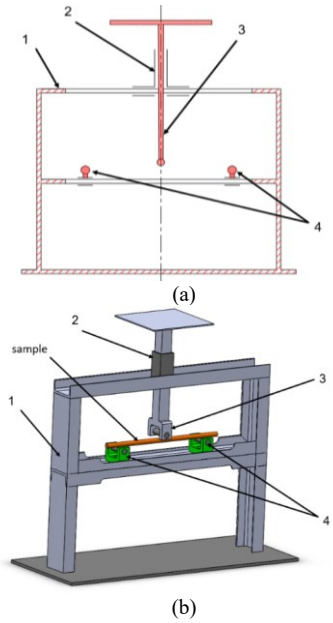

Fig. 1. (a) Diagram of the testing device;
(b) The 3D CAD model
1: Chassis- 2: Rail- 3: Loading block- 4: Two supports

Developed in Solidworks CAD software [13] (Fig. 1b), the 3-point bending test apparatus was subsequently manufactured and assembled (Fig. 2). A linear variable displacement transducer (LVDT) positioned at the beam's midpoint facilitated accurate displacement measurement during experimentation.

Fig. 2. The actual device.

B. Three-Point Bending Test

The template is used to format your paper and style the text. All margins, column widths, line spaces, and text fonts are prescribed; please do not alter them. You may note peculiarities. For example, the head margin in this template measures proportionately more than is customary. This measurement and others are deliberate, using specifications that anticipate your paper as one part of the entire proceedings, and not as an independent document. Please do not revise any of the current designations.

1. Beam bending test based on theory of material strength

The employed model leverages the double integration method, which involves applying the moment-curvature equation (a second-order derivative formula defining curvature) alongside specified boundary conditions. It initially calculates the deflection of a cantilever beam model, which subsequently serves as the foundation for determining deflection in the 3-point bending beam scenario. The calculations adhere to the guidelines outlined in [11]. In Fig. 3, L: length of beam; F: applied force; δ: displacement vertical; M: moment.

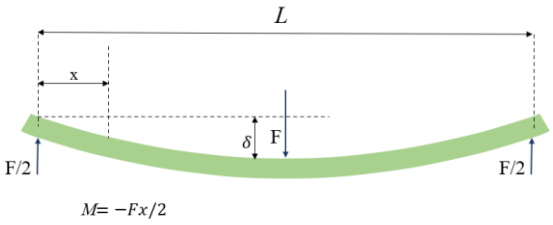

Fig. 3. Deformation model of 3-point bending beam.

For 3-point bending model, we calculate:
Displacement equation:

$$y = \frac{Fx}{48EI}(3L^2 - 4x^2) \quad (1)$$

Maximum displacement at x = $\frac{L}{2}$:

$$y_{max} = \delta = \frac{FL^3}{48EI} \quad (2)$$

2. Beam bending test based on finite element method

For 3-point bending beam, to calculate theoretically, it can be divided into 2 elements and 3 nodes is shown in Fig. 4.

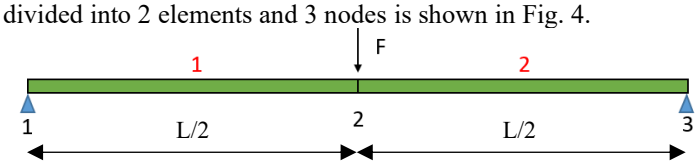

Fig. 4. The beam was divided into 2 elements and 3 nodes.

Published by :
http://www.ijert.org

International Journal of Engineering Research & Technology (IJERT)
ISSN: 2278-0181
Vol. 13 Issue 4, April 2024

The beam was divided into 2 elements; each element has the deformation type as a cantilever beam having a stiffness k;

Stiffness matrix of each element:

$$[k_1]=\frac{E.I}{(\frac{L}{2})^3}\begin{bmatrix}12 & 6(L/2) & -12 & 6(L/2)\\ 6(L/2) & 4(\frac{L}{2})^2 & -6(L/2) & 2(\frac{L}{2})^2\\ -12 & -6(L/2) & 12 & -6(L/2)\\ 6(L/2) & 2(\frac{L}{2})^2 & -6(L/2) & 4(\frac{L}{2})^2\end{bmatrix} \quad (3)$$

$$[k_2]=\frac{E.I}{(\frac{L}{2})^3}\begin{bmatrix}12 & 6(L/2) & -12 & 6(L/2)\\ 6(L/2) & 4(\frac{L}{2})^2 & -6(L/2) & 2(\frac{L}{2})^2\\ -12 & -6(L/2) & 12 & -6(L/2)\\ 6(L/2) & 2(\frac{L}{2})^2 & -6(L/2) & 4(\frac{L}{2})^2\end{bmatrix} \quad (4)$$

Global stiffness matrix:

$$[K]=\frac{E.I}{(\frac{L}{2})^3}\begin{bmatrix}12 & 6(L/2) & -12 & 6(L/2) & 0 & 0\\ 6(L/2) & 4(\frac{L}{2})^2 & -6(L/2) & 2(\frac{L}{2})^2 & 0 & 0\\ -12 & -6(L/2) & 24 & 0 & -12 & 6(L/2)\\ 6(L/2) & 2(\frac{L}{2})^2 & 0 & 8(\frac{L}{2})^2 & -6(L/2) & 2(\frac{L}{2})^2\\ 0 & 0 & -12 & -6(L/2) & 12 & -6(L/2)\\ 0 & 0 & 6(L/2) & 2(\frac{L}{2})^2 & -6(L/2) & 4(\frac{L}{2})^2\end{bmatrix} \quad (5)$$

Boundary conditions:

- Displacement at fulcrums equals 0

$$[Y]=\begin{bmatrix}u_{y1}\\ \theta_1\\ u_{y2}\\ \theta_2\\ u_{y3}\\ \theta_3\end{bmatrix} \quad (6)$$

- Reactive force at fulcrums:

$$[F]=\begin{bmatrix}F_1\\ M_1\\ F_2\\ M_2\\ F_3\\ M_3\end{bmatrix} \quad (7)$$

The relating global equation:

$$[F]=[K]*[Y] \quad (8)$$

3. Finite element modeling in Abaqus ® CAE

The CAE simulation model for the 3-point bending beam is computed using the finite element method theory. Abaqus® software [14] is employed in this study to simulate both 2D and 3D models. For the 2D beam models, the reduced number of elements facilitates easier and faster model construction and calculation compared to 3D models. A concentrated force F (N) is applied at the center point of the beam (Fig. 5).

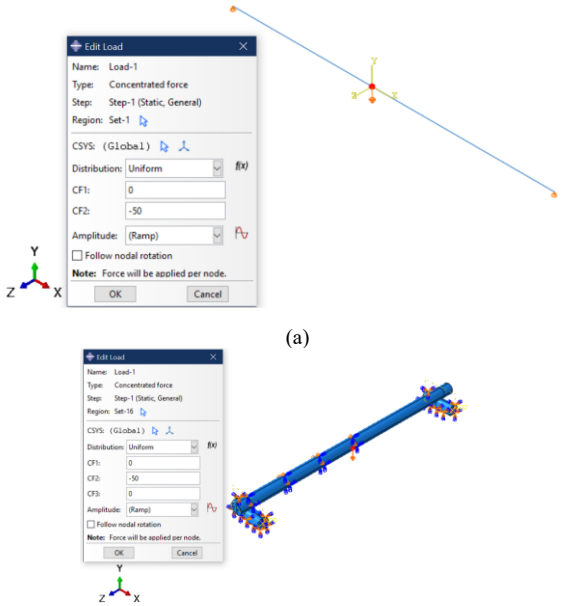

(a)

(b)

Fig. 5. Locate concentrated load of 50N: (a) for model beam 2D and (b) for model beam 3D.

At the two supports, following the theory of bending beam deformation, the beam undergoes bending under ideal conditions. In the coordinate system depicted in Fig. 6, these two points exclusively rotate around the z-axis and move along the x-axis. As illustrated in the Fig. 6b, each of these two points is constrained with four degrees of freedom.

Published by :
http://www.ijert.org

International Journal of Engineering Research & Technology (IJERT)
ISSN: 2278-0181
Vol. 13 Issue 4, April 2024

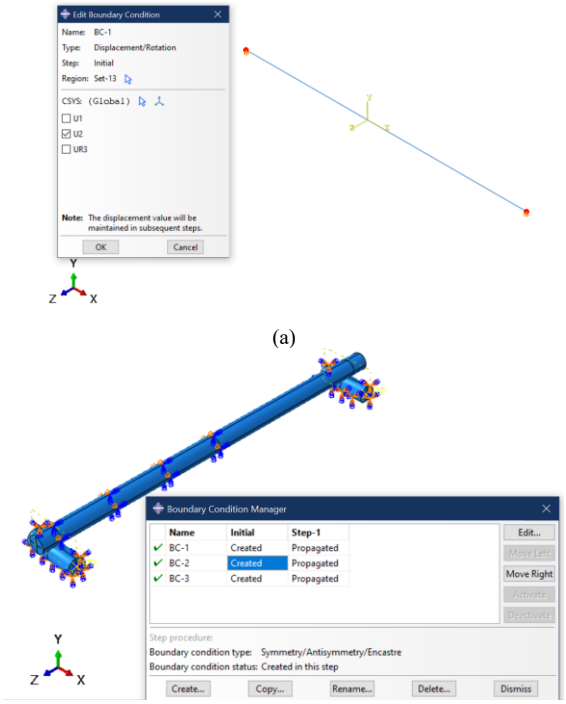

(a)

(b)

Fig. 6. Setting boundary condition: (a) for model beam 2D and (b) for model beam 3D.

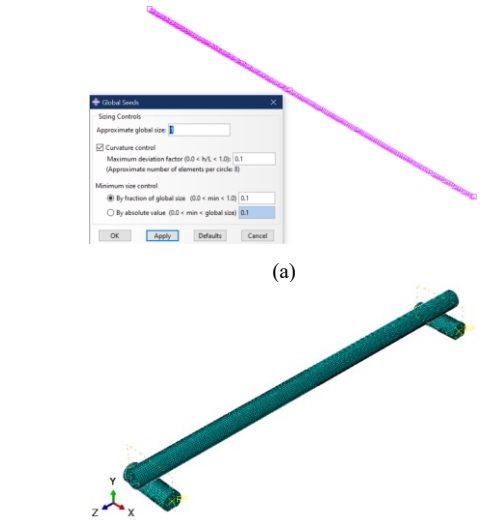

(a)

(b)

Fig. 7. Model finite element (mesh) with size element 1mm: (a) for model beam 2D and (b) for model beam 3D (d=10mm)

C. Experiments

The experiments were carried out using a circular-section beam made of A6061 aluminium (Fig. 8a). All the samples used for experimental calculations and simulations had a bent section length of L = 200 mm. These samples featured circular cross-sections with diameters of 6 mm, 8 mm, and 10 mm, respectively. The physical and mechanical properties of A6061 is described in Table 1. Each beam was subjected to four different load values: 50N, 70N, 90N, and 110N on the custom-designed 3-point bending device (Fig. 8b).

The mesh size for the numerical model was selected by assessing mesh convergence for element sizes of 0.5, 0.75, and 1 mm, respectively. For the example test case with a model diameter d of 6 mm and a load of 50 N, the maximum error observed was 4.7% for mesh sizes of 0.75 mm and 1 mm, while the minimum error was 2.2% for mesh sizes of 0.5 mm and 1 mm. Consequently, a mesh size of 1 mm was chosen for conducting numerical simulations in this study (see Fig. 7). In finite element models, computer-assisted calculations are significantly faster than manual calculations. Meshing for the 2D model is easier compared to the 3D model. For the 3D beam model, dimensional parameters, boundary conditions, and loads were identical to those used in manual calculations and 2D simulations. In the 3D model, two supports were designed to replicate the shape of those used in the actual experiments, featuring a cylindrical shape with a diameter of d=10 mm. These two supports were constrained with 6 degrees of freedom in space. To enhance stability in calculations, constraints were applied to the beam to prevent rotation around the z-axis and y-axis, as well as movement along the x-axis. The 3D beam was meshed using the linear element type Hexahedral C3D8R, with a size of 1 mm for each element.

TABLE 1. PHYSICAL AND MECHANICAL PROPERTIES OF A6061 [12]

Physical Properties	**Metric**
Density	2.7 g/cm^3
Mechanical Properties	
Hardness, Brinell	95
Hardness, Knoop	120
Hardness, Rockwell A	40
Hardness, Rockwell B	60
Hardness, Vickers	107
Ultimate Tensile Strength	310 MPa
Tensile Yield Strength	276 MPa
Elongation at Break	12 %
Elongation at Break	17 %
Modulus of Elasticity	68.9 GPa
Notched Tensile Strength	324 MPa
Ultimate Bearing Strength	607 MPa
Bearing Yield Strength	386 MPa
Poisson's Ratio	0.33
Fatigue Strength	96.5 MP

International Journal of Engineering Research & Technology (IJERT)
ISSN: 2278-0181
Vol. 13 Issue 4, April 2024

(a)

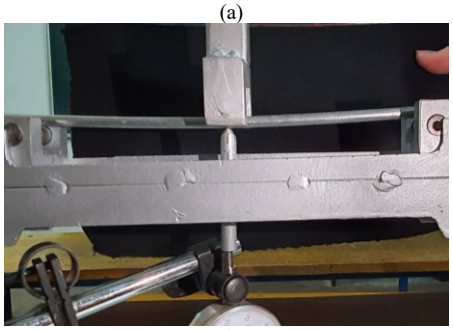

(b)

Fig. 8. (a) Aluminium samples and (b) testing on the actual device.

III. RESULTS AND DISCUSSION

Theoretical calculations based on strength of materials principles and finite element analysis (FEA) were both conducted within the MATLAB ® software environment [15], yielding remarkably consistent displacement results. After performing calculations using these two methods, we compared them to the simulation results obtained by Abaqus®. The 2D simulation and 3D simulation, involving a circular-section beam with a diameter of d=6 mm, are shown in Fig. 9, respectively.

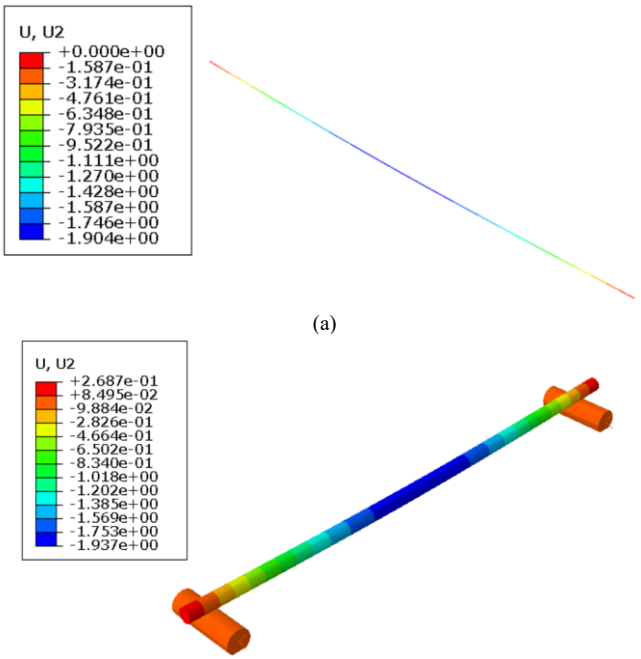

Fig. 9. (a) 2D simulation results for an aluminium sample with a diameter of d=6 mm, load F=50N; (b) 3D simulation results for an aluminium sample with a diameter of d=6 mm, load F=50N

Subsequently, experiments were conducted, and displacements were measured using an indicator with an accuracy of 0.01 mm. The results of calculations, simulations, and experiments for aluminium samples with circular cross-sections are summarized in Table 2:

TABLE 2. DISPLACEMENT RESULTS FROM CALCULATION, SIMULATION, AND EXPERIMENTATION FOR AN ALUMINIUM CIRCULAR CROSS-SECTION BEAM (IN MM)

Diameter (mm)	**Load (N)**	**Calculation**	**Simulation**		**Experimental** *(Average result of three measurements)*
			2D	**3D**	
d = 6	50	1.9012	1.904	1.936	1,86
	70	2.6617	2.665	2.71	2,57
	90	3.4222	3.425	3.486	3,32
	110	4.1826	4.184	4.266	4,15
d = 8	50	0.6016	0.6037	0.5803	0,56
	70	0.8422	0.8451	0.805	0,75
	90	1.0828	1.087	1.03	0,98
	110	1.3234	1.328	1.255	1,18
d = 10	50	0.2464	0.2478	0.2406	0,25
	70	0.3450	0.3469	0.3303	0,34
	90	0.4435	0.446	0.4201	0,43
	110	0.5421	0.5451	0.5099	0,53

International Journal of Engineering Research & Technology (IJERT)
ISSN: 2278-0181
Vol. 13 Issue 4, April 2024

With the collected calculation, simulation, and experimental results, it can be affirmed that the research has successfully achieved its initial goals. The calculation and simulation results demonstrated a high level of accuracy when compared to the experimental findings, particularly in the elastic deformation region where the sample made of Aluminium A6061 exhibited linear deformation. The displacement calculation results, obtained through theoretical methods and 2D simulations, show very small deviations, with a maximum deviation of about 0.01 mm (Tab. 2). Meanwhile, the displacement calculation results based on 3D simulations reveal larger errors, with a maximum deviation of about 0.05 mm. It can be easily observed that the displacement measured in experiments is larger than the results obtained from theoretical calculations and simulations. However, across all samples and loads, the differences between experiments and 3D simulations were generally small, ranging from a minimum of 1.82% to a maximum of 5.93% (between FEM and 3D model) and of 2.36% to a maximum of 6.83% (between 3D model and Experimental). The most significant difference occurred in the case of a sample with a diameter of d = 6 mm and a load F = 110 N, where plastic deformation occurred beyond the elastic limit, leading to a shape change after unloading. Apart from this exceptional case, the differences in the remaining scenarios ranged from 0% to 4%. The displacement in relation to different loads, determined through theoretical calculations, 2D and 3D simulations, as well as experimental measurements for test specimens with diameters of 6mm, 8mm, and 10mm, is shown in Fig. 10.

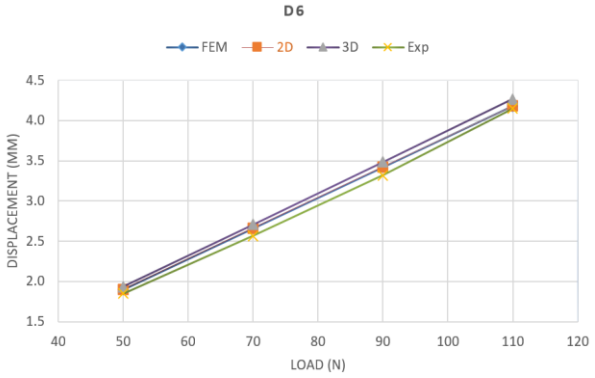

(a)

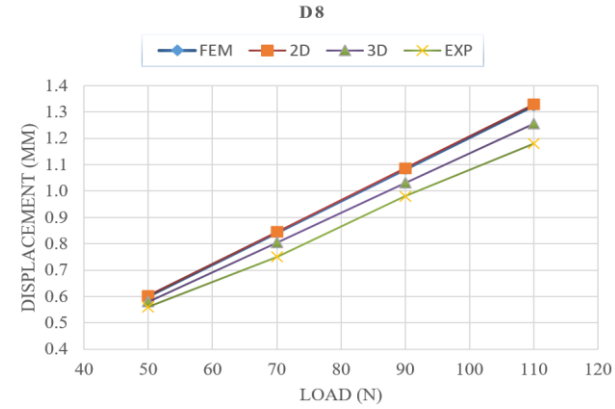

(b)

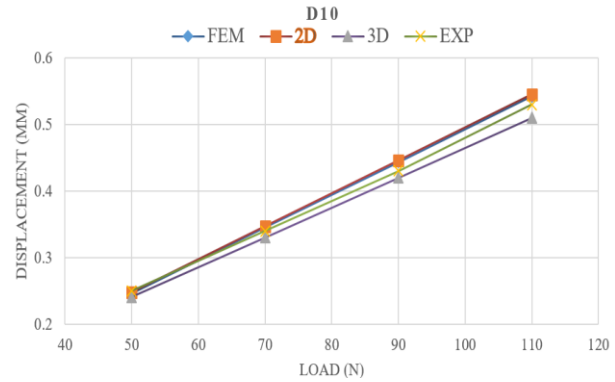

(c)

Fig. 10. (a) Displacements of sample with a diameter = 6 mm (b) diameter = 8mm and (c) diameter = 10mm

International Journal of Engineering Research & Technology (IJERT)
ISSN: 2278-0181
Vol. 13 Issue 4, April 2024

IV. CONCLUSIONS

In this paper, the deflection behavior of aluminium alloy A6061 has been tested using three methods analytical calculations based on the strength of materials theory, finite element simulations, and experimental measurements on a custom-designed 3-point flexural test device. The accuracy of the calculation and simulation results was evident, especially in the elastic deformation region, where Aluminium A6061 sample displayed linear deformation, as observed in comparison to the experimental findings.

According to the study results, the prediction of displacement in load-bearing samples through calculation and simulation methods proved to be highly accurate. Consequently, it can be asserted that predicting various physical quantities such as stress and strain through these methods is reliable. Several factors influenced the accuracy of calculation and simulation. Firstly, the properties of the material used must be consistent with those of real samples. Secondly, during simulation, it is crucial to accurately set the load and boundary conditions to match real circumstances, and the meshes should be appropriately divided. Thirdly, the testing equipment must meet the accuracy requirements.

In practice, numerical simulation stands out as a useful and credible method with minimal error. When dealing with complex parts, theoretical calculation methods may not suffice for evaluating or predicting displacement, stress, and strain. In such cases, the finite element method becomes a pivotal solution for approximating results. By relying on several simple simulation models, one can identify the most accurate model for the material sample. The criteria, data, and methods of this model can be further developed and applied to mesh division and simulate complex models.

ACKNOWLEDGMENT

This research is funded by The University of Danang – University of Technology and Education under project number T2022-06-10.

REFERENCES

[1] E. Georgantzia, M. Gkantou, and G. S. Kamaris, “Aluminium alloys as structural material: A review of research,” Engineering Structures, vol. 227, p. 111372, 2021.
[2] M.-N. Su, B. Young, and L. Gardner, “Deformation-based design of aluminium alloy beams,” Engineering structures, vol. 80, pp. 339–349, 2014.
[3] R. Montuori, E. Nastri, V. Piluso, and A. Pisapia, “Ultimate behaviour of high-yielding low-hardening aluminium alloy I-beams,” Thin-Walled Structures, vol. 146, p. 106463, 2020.
[4] V. Piluso, A. Pisapia, E. Nastri, and R. Montuori, “Ultimate resistance and rotation capacity of low yielding high hardening aluminium alloy beams under non-uniform bending,” Thin-Walled Structures, vol. 135, pp. 123–136, 2019.
[5] P. Castaldo, E. Nastri, and V. Piluso, “Ultimate behaviour of RHS temper T6 aluminium alloy beams subjected to non-uniform bending: Parametric analysis,” Thin-Walled Structures, vol. 115, pp. 129–141, 2017.
[6] Y. Kim and T. Peköz, “Numerical Slenderness Approach for design of complex aluminium extrusions subjected to flexural loading,” Thin-Walled Structures, vol. 127, pp. 62–75, 2018.
[7] R. Feng, Z. Chen, C. Shen, K. Roy, B. Chen, and J. B. Lim, “Flexural capacity of perforated aluminium CHS tubes–An experimental study,” in Structures, Elsevier, 2020, pp. 463–480.
[8] M.-N. Su, B. Young, and L. Gardner, “Flexural response of aluminium alloy SHS and RHS with internal stiffeners,” Engineering Structures, vol. 121, pp. 170–180, 2016.
[9] P. Hou et al., “Influence of punch radius on elastic modulus of three-point bending tests,” Advances in Mechanical Engineering, vol. 8, no. 5, p. 1687814016649116, 2016.
[10] D. Jindra, Z. Kala, J. Kala, and S. Seitl, “Experimental and numerical simulation of a three-point bending test of a stainless steel beam,” Transportation Research Procedia, vol. 55, pp. 1114–1121, 2021.
[11] University of Cambridge, “Beam deflections from applied bending moments, Dissemination of IT for the Promotion of Materials Science, University of Cambridge.” [Online]. Available: https://www.doitpoms.ac.uk/tlplib/beam_bending/beam_deflection.php (accessed: March 25, 2024).
[12] “ASM International: ASM Aerospace Specification Metals Inc. Aluminium 6061-T6; 6061-T651[Internet]. Materialsre Park (OH): American Society of Materials; c1913-2017.” Accessed: Dec. 29, 2023. [Online]. Available: https://asm.matweb.com/search/SpecificMaterial.asp?bassnum=MA6061t6
[13] Solidworks ® CAD software.
[14] ABAQUS® CAE, Version 6.13.
[15] MATLAB ® software environment.